Geophysical Research Letters

RESEARCH LETTER
10.1029/2019GL083453

A Multivariate Approach for Mapping Lithospheric Domain Boundaries in East Antarctica

Tobias Stål[1,2], Anya M. Reading[1,2], Jacqueline A. Halpin[2], and Joanne M. Whittaker[2]

[1]School of Natural Sciences (Earth Sciences), University of Tasmania, Hobart, Tasmania, Australia, [2]Institute for Marine and Antarctic Studies, University of Tasmania, Hobart, Tasmania, Australia

Key Points:
- Use of geophysical data to constrain lithospheric domain boundaries
- A novel multivariate and probabilistic approach is introduced
- Newly inferred segmentation of the East Antarctic lithosphere

Supporting Information:
- Supporting Information S1
- Text S1
- Text S2
- Figure S1
- Figure S2
- Figure S3
- Figure S4
- Figure S5
- Figure S6

Correspondence to:
T. Stål,
tobias.staal@utas.edu.au

Citation:
Stål, T., Reading, A. M., Halpin, J. A., & Whittaker, J. M. (2019). A multivariate approach for mapping lithospheric domain boundaries in East Antarctica. *Geophysical Research Letters*, *46*, 10,404–10,416. https://doi.org/10.1029/2019GL083453

Received 24 APR 2019
Accepted 22 AUG 2019
Accepted article online 27 AUG 2019
Publishedonline 10 SEP 2019

Abstract Beneath the ice of East Antarctica lies a continent that is likely to be as geologically complex as its neighbors in Gondwana. An improved model of the heterogeneous lithosphere is required to progress research on Antarctica's tectonic evolution and support interdisciplinary studies of cryosphere and solid Earth interaction. We make use of multiple data sets, which were updated following the field campaigns and compilations of the International Polar Year of 2007/2008. Seismic tomography results, gravity anomalies, and surface elevation are used in a novel method, which combines spatial multivariate data to map possible boundaries as projected likelihood functions. Six multivariate combinations are tested and compared with sparse geological observations in East Antarctica. The resulting lithospheric domain boundaries contribute to our understanding of the deep continental structure. New boundaries are suggested in the interior, and models agree with likely surface expressions of crustal tectonic boundaries exposed along the coast.

1. Introduction

Important aspects of Antarctica's continental structure are unknown. Better working models of the deep lithosphere are needed to progress investigations of the complex interaction between the solid Earth and the cryosphere. For example, glacial isostatic adjustment in response to changes in ice load depends on deep elastic and viscous properties (e.g., Kaufmann et al., 2005; Whitehouse, 2018; Whitehouse et al., 2006). Geothermal heat is identified as a spatially variable and poorly constrained parameter in ice sheet models (e.g., Burton-Johnson et al., 2017; Pollard et al., 2005). Deep boundaries subdivide the continental lithosphere into domains with similar physical properties. With a more detailed and robust map of lithospheric boundaries and domains, we can better infer the tectonic evolution of the continent and assign physical properties to provide a useful framework for interdisciplinary studies.

The main crustal domains in East Antarctica were identified along the perimeter and Transantarctic Mountains from geological observations by the 1980s, but no constraints were available for the subglacial interior (e.g., Craddock, 1972; Ravich et al., 1965; Tingey, 1991). Indirect observations of transported material from marine cores and moraines can suggest the large-scale hidden geology (Cook et al., 2017; Goodge, 2018; Tauxe et al., 2015), but the provenance of samples can be difficult to reconstruct. Some studies have projected coastal geology into the unexposed interior. Those predictions have been guided by extrapolation of known geology from adjacent Gondwanan neighbors or by using geophysical data (e.g., Aitken et al., 2014; Boger, 2011; Daczko et al., 2018; Ferraccioli et al., 2011; Fitzsimons, 2003; Jacobs et al., 2015; Veevers, 2012). Over the past decades, geophysical studies and plate reconstructions have advanced the understanding of Antarctica's continental structure, but there are still conflicting interpretations of the blocks and boundaries in the interior (Figure 1a).

We rely on geophysical data to map East Antarctica, and different data sets have particular strengths and limitations. Early seismic tomography studies revealed general heterogeneities within the lithosphere (Ritzwoller et al., 2001; Roult & Rouland, 1994; Roult et al., 1994). There were, however, few seismometers in Antarctica at this time and seismic tomography using local sources is precluded due to the inherent low seismicity (Reading, 2007). Global studies provide a reference but are often of low resolution due to the limited data for Antarctica (Laske et al., 2013; Pasyanos et al., 2014; Ritzwoller et al., 2002; Schaeffer & Lebedev, 2015; Shapiro & Ritzwoller, 2002). Transects and regional studies have revealed the basement structure of the Transantarctic Mountains, Lambert Glacier region, Gamburtsev Subglacial Mountains, and West Antarctica (e.g., Chaput et al., 2014; Gregory et al., 2017; Hansen et al., 2010; Heeszel et al., 2016;

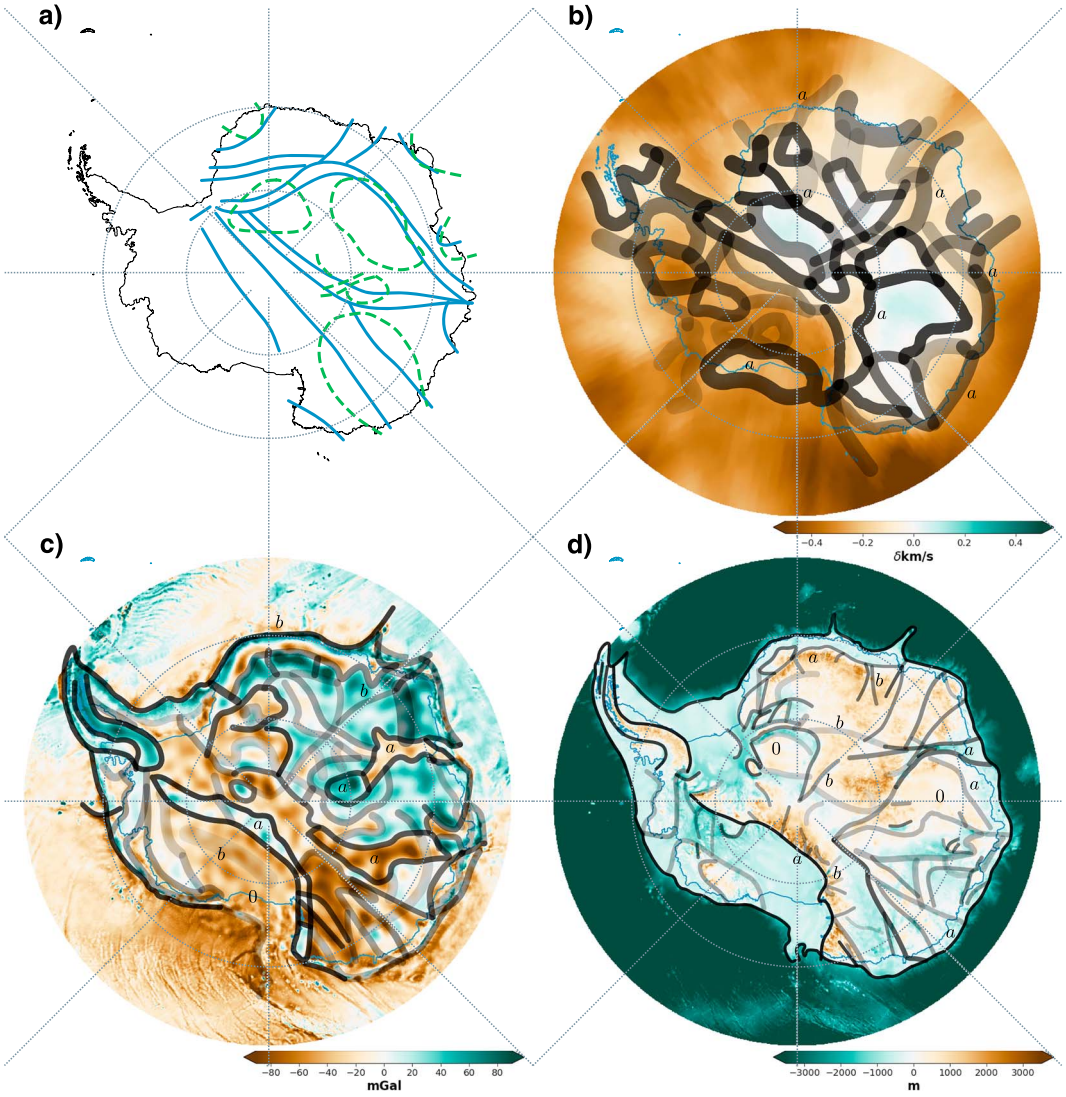

Figure 1. (a) Sketches of major boundaries suggested in previous studies and compilations. Blue solid lines (e.g., Boger, 2011), the continent defined as an extrapolation from the Gondwanan and Rodinian neighbors, or lack of such candidates. Green dashed lines (e.g., Leitchenkov et al., 2016), Antarctica as an unknown entity with mainly inferred geophysical properties. (b–d) Data sets used for this study and picked boundaries (black lines). Opacity illustrates the relative accuracy and line widths indicate precision. (b) Seismic shear wave speed at 150 km as perturbation from AK135 in absolute speed anomaly, modified from An et al. (2015a). (c) Gravity anomaly map EIGEN-6C4, modified from Förste et al. (2014). (d) Bed elevation model BEDMAP2 modified from Fretwell et al. (2013). Examples of detected boundaries are notated *a* for changes in value, *b* for changes in pattern; 0 indicates examples of artifacts that are not interpreted.

Jordan et al., 2017; Reading, 2006; Shen et al., 2017, 2018; Winberry & Anandakrishnan, 2004). An et al. (2015a, 2015b) presented an improved surface wave tomography model that is used to estimate crustal thickness, temperature, and lithospheric thickness. Teleseismic surface wave tomography captures the character of lithospheric blocks in the centers of domains but is less suited to the detection of their boundaries (An, 2012; Foulger et al., 2013). The edges of gravity anomalies are valuable in revealing boundaries between lithospheric domains (Block et al., 2009; Ferraccioli et al., 2011), but interpretation can be ambiguous and the resolution is often low. Gravity data can be obtained from ground measurements, airborne instruments, and by satellite. GOCE and GRACE (Gravity Field and Steady-state Ocean Circulation Explorer and Gravity Recovery and Climate Experiment) satellite missions have been important in Antarctica (Pail et al., 2010; Visser, 1999). Variations in bedrock topography can to some extent provide indication of much deeper

structure. In Antarctica, there are few direct observations. Instead, topography is inferred from, for example, airborne radar surveys (Fretwell et al., 2013). Finer-scale features of topography may not be captured in interpolated elevation models (Graham et al., 2017).

Geological and geochronological information have sparse coverage in East Antarctica, but good resolution. Geophysical data sets might have good coverage, but often limited resolution. Combined geological and geophysical studies to map and constrain the lithospheric structure has been conducted in Africa (e.g., Begg et al., 2009) and Australia (e.g., Kennett et al., 2018). The lithospheric domains in those continents suggest what we could expect to infer in Antarctica as data availability improves.

In this study, we introduce a novel method to identify domain boundaries in the lithosphere of Antarctica, with a focus on East Antarctica. In contrast to previous studies, which make interpretations based on a comparative analysis of univariate data, we use a multivariate interpretation of the relative probability of inferred boundaries. We map variations in geophysical observables that suggest deep boundaries or transitions. The new domain maps aim to progress the understanding of the large-scale tectonic structure of the interior of East Antarctica.

2. Data

To place constraints on domain boundaries within the lithosphere, we utilize three data sets: seismic shear wave speed (S), free air gravity anomaly (G), and subglacial elevation (E). Data set selection is based on reasonably consistent resolution across East Antarctica. The seismic data set used is the 150-km depth slice from An et al. (2015a). Beneath East Antarctica, this depth is mainly within the lower lithosphere, which is the focus of this study. Beneath West Antarctica and parts of coastal East Antarctica, we note that this depth falls below the lithosphere-asthenosphere boundary. Gravity anomalies are taken from the Earth free air gravity model EIGEN-6C4 compilation. This data set includes GRACE and GOCE data up to degree and order 2190 (Förste et al., 2014). In order to keep the data sets independent, we avoid the use of a Bouguer-corrected gravity model, which incorporates the effects of topography. Subglacial elevation is taken from the digital elevation model BEDMAP2 (Fretwell et al., 2013). The data sets were prepared for analysis by reprojection, resampling, and clipping using, for example, the Python package rasterio (Gillies, 2018). The seismic data are replotted using a diverging color map (Figure 1b) as a perturbation from AK135 shear wave speed model at 150 km, 4.5060 km/s (Kennett, 2005). Gravity and elevation data are replotted as obtained from original data sources.

3. Methods

3.1. Picking Boundaries

For each data set, boundaries are independently identified visually and manually picked as vector lines in a GIS software environment (QGIS, 2015). Effort is made by the analyst not to be biased by previous knowledge or other data sets. Rapid changes or obvious changes in trends are selected as boundaries (examples notated *a* in Figures 1b–1d). Changes in pattern, particularly for the gravity and elevation data sets, are also taken to indicate a domain boundary (examples notated *b* in Figures 1b–1d). The lines are not picked to be geological meaningful; they represent visual variations in the data. Known and obvious artifacts, such as flight lines, are avoided (examples notated 0 in Figures 1b–1d). Some boundaries fade out to become obscure and are only mapped as far as they are traceable. Boundary identification is carried out on a map screen display, which uses an Antarctic Polar Stereographic projection and shows minimal scalar distortion in continental Antarctica.

Each picked line segment is associated with relative accuracy and precision ratings. The accuracy rating represents the certainty of the picked line representing a lithospheric boundary. The precision is the spatial uncertainty of the picking. Both ratings are given as a number between 1 and 10 and later converted to likelihood value from 0 to 1, and standard deviation expressed as a distance.

3.2. Generating Individual Spatial Likelihood Maps

For each data set, D, we calculate a likelihood map representing the picked boundaries as follows:

$$\mathcal{L}(x,y)_D = a_D \sum_{s(x,y)\in L'_D} a_s \times s(x,y) * \mathcal{N}_2\left(\mu(x,y), (\sigma_s + \sigma_D)^2\right). \quad (1)$$

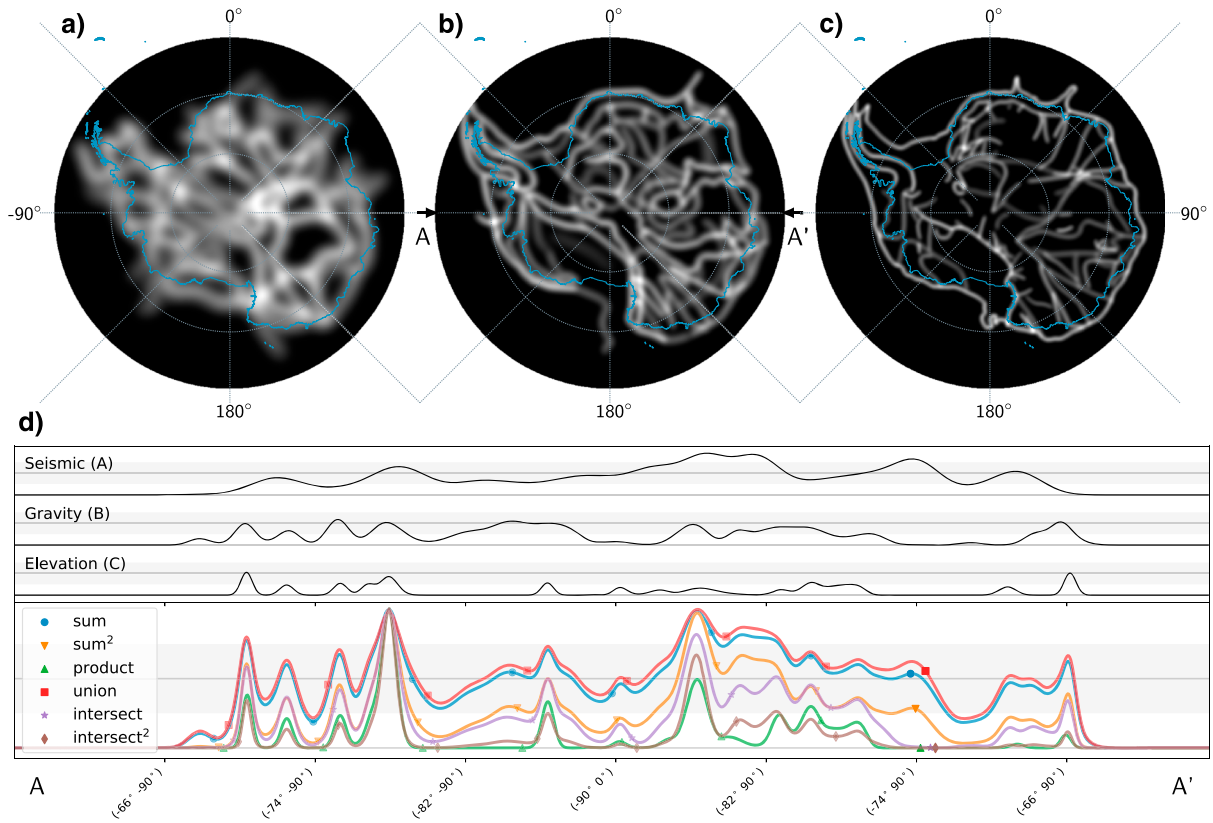

Figure 2. Likelihood maps of domain boundaries for each geophysical data set used, here normalized to the maximum value within each data set. Brighter shading indicates a higher likelihood of a domain boundary. (a) Seismic derived boundary likelihood map. (b) Free air gravity derived boundary likelihood map. (c) Elevation derived boundary likelihood map. (d) Cross-section (A-A'), showing convolved distributions for likelihood of boundary from each data set and combined distributions, as described in text.

where $\mathcal{L}(x, y)$ is the spatial likelihood function, projected to a (x, y) Polar Stereographic grid. $s(x, y)$ denotes the location of the line segments in the picked vector lines, L'; a_D is the weighting for the boundaries for each data set, and a_s is the accuracy rating for each picked line segment. $\mathcal{N}_2(\mu, \sigma^2)$ is a two-dimensional Gaussian kernel, with $\mu(x, y) = (0, 0)$ and $\sigma = \sigma_s + \sigma_D$, where σ_s is a function of the user-defined precision rating for each line segment and σ_D is the standard deviation for the data set used; a_s and σ_s are stored as attribute data in the vector file (L').

The width of the Gaussian kernel relating to the seismic data is indicated by the tomography methodology and data density (An, 2012; Ritsema et al., 2004). At 150-km depth, periods of over 100 s dominate and for most of continental Antarctica the resolution of features in the tomogram is in the range 300–500 km (An et al., 2015a). The picked seismic boundaries are convolved with a Gaussian kernel with a standard deviation $\sigma_S = 200$ km (Figure 2a). The gravity field model EIGEN-6C4 has an estimated half-width resolution of $\Delta \approx 80$ km. The Antarctic interior has increased uncertainty due to the lack of ground-based observation data. The picked gravity boundaries are convolved with a standard deviation $\sigma_G = 100$ km (Figure 2b). The horizontal resolution of the digital elevation model (Fretwell et al., 2013) is 1 km, but the data in some areas are coarser due to the acquisition methods. For the picked topography boundaries, a Gaussian convolution with a standard deviation of $\sigma_E = 60$ km is applied to also account for sloping crustal structures (Figure 2c).

The relative amplitude of the Gaussian kernel for each of the three data sets is the product of the total weight for the data set and the weights for the segments of the picked boundaries. We assign equal weight ($a_D = 0.33$) to each likelihood function.

3.3. Combining Distributions

We demonstrate six methods of combining individual likelihood maps (Figures 2d and 3). Sum (Figure 3a) is generated by adding the three map values for each grid cell. Product (Figure 3e) is generated by multiplying the three map values for each grid cell. Union (Figure 3b) and intersect (Figure 3d) are achieved from

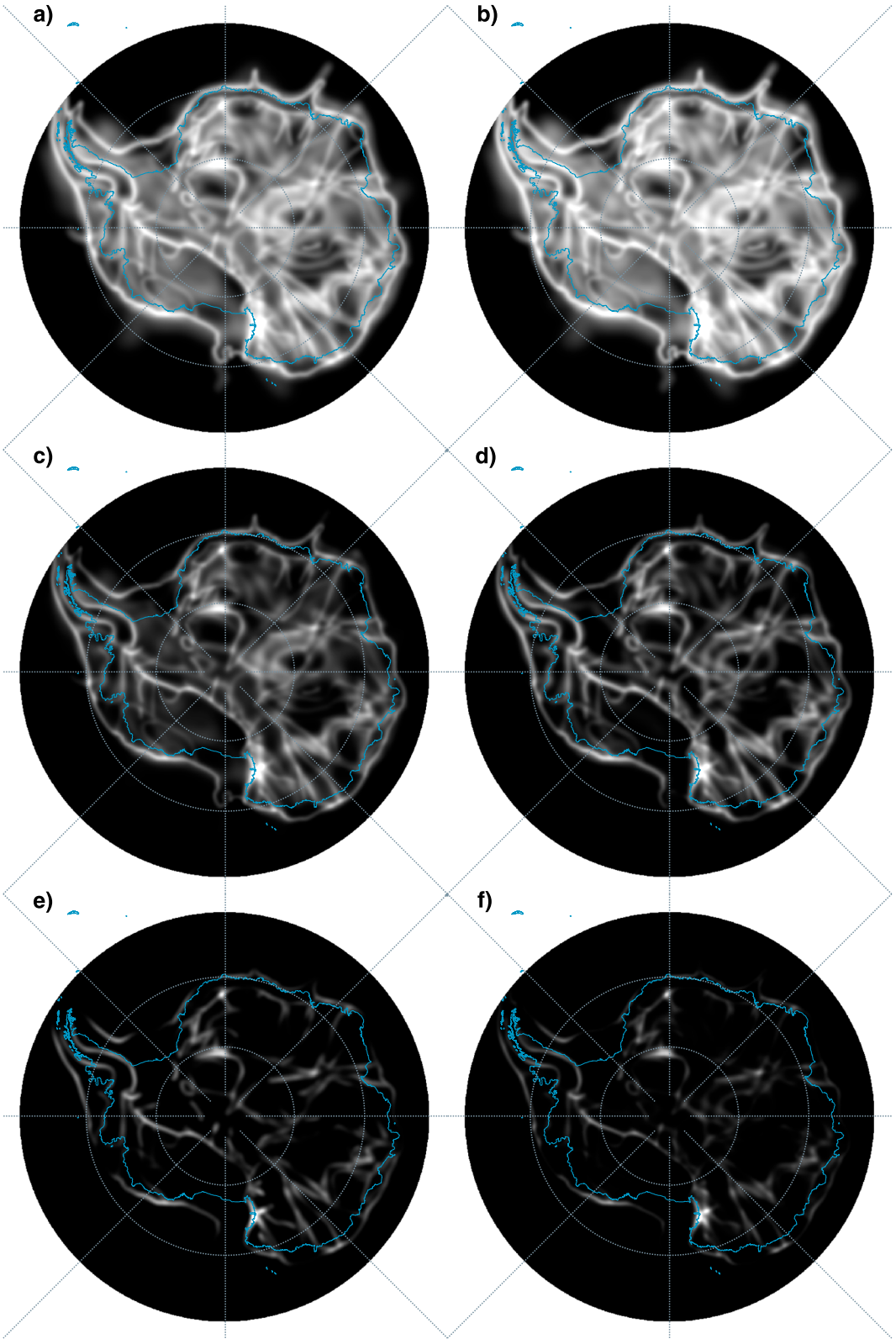

Figure 3. Combined likelihood maps, generated using six different methods: (a) sum, (b) union, (c) squared sum, (d) intersect, (e) product, and (f) squared intersect. Each map is normalized to the maximum value for each combination.

the inclusion-exclusion principle (Brualdi, 1992). In our simple case with only three sets of independent distributions, we make the following calculation for union:

$$\mathcal{L}_S \cup \mathcal{L}_G \cup \mathcal{L}_E = \mathcal{L}_S + \mathcal{L}_G + \mathcal{L}_E - (\mathcal{L}_S \times \mathcal{L}_G + \mathcal{L}_S \times \mathcal{L}_E + \mathcal{L}_G \times \mathcal{L}_E) + \mathcal{L}_S \times \mathcal{L}_G \times \mathcal{L}_E. \quad (2)$$

and a similar calculation for intersect:

$$\mathcal{L}_S \cap \mathcal{L}_G \cap \mathcal{L}_E = \mathcal{L}_S \times \mathcal{L}_G + \mathcal{L}_S \times \mathcal{L}_E + \mathcal{L}_G \times \mathcal{L}_E - \mathcal{L}_S \times \mathcal{L}_G \times \mathcal{L}_E. \quad (3)$$

Squared sum (Figure 3c) and squared intersect (Figure 3f) emphasize the regions of highest likelihood of a boundary. We note that the combined likelihood is not a joint probability distribution as the projected axes represent spatial extent, not separate distributions. Figure 2d shows transects across the probability fields along the 90°W and 90°E meridians through the South Pole. For clarity, each field is normalized according to its maximum value.

4. Results

Of the six resulting likelihood maps derived from the multivariate approach (Figure 3), sum (a) and union (b) are the method combinations that suggest the highest number of likely boundaries. An intermediate result is given by squared sum (c) and intersect (d). The most conservative results, suggesting fewest lithospheric boundaries, are product (e) and squared intersect (f). Conservative combinations indicate high likelihood for the existence of actual lithospheric boundaries with reduced false positive detection. The maps suggest high likelihood for lithospheric boundaries along the Transantarctic Mountains and subparallel to the coast in Dronning Maud Land (geographical locations are given in Figure 4). The lithosphere appears most heterogeneous, showing high likelihood of intersecting boundaries, in the region of Coats Land and Shackleton Range. In contrast, regions with lower likelihood of major lithospheric boundaries are suggested within Wilkes Land, Princess Elizabeth Land and around the South Pole. In the discussion that follows, we use the intermediate results, intersect (d). However, the range of maps is also informative. An analysis of shallower neotectonic features in West Antarctica is beyond the scope of this contribution. With the data sets used in this study, we capture only the most deep-seated lithospheric boundaries in West Antarctica.

5. Discussion

5.1. Limitations

Our objective is to define domain boundaries in the deep lithosphere. Crustal domains might be different. We acknowledge that the different data sets used are sensitive to structure at differing depths and differing depth ranges. Further, the different data sets may not reconcile with each other. Embedded in these data are information on the upper crust and recent geomorphology. Hence, our method has an inherent assumption that all major lithospheric boundaries may be approximated as vertical. As more detailed 3-D studies of the lithosphere are carried out in the future, we expect this assumption to be refined. The 150-km depth slice from seismic tomography is within the asthenosphere in some parts of continental Antarctica. Our model does not capture West Antarctic lithospheric domain boundaries but indicates the presence of the lithosphere-asthenosphere boundary. We note that more detailed seismic tomography studies are available (e.g., Shen et al., 2018), which could constrain upper lithosphere segmentation for the given study region, using the methods that we introduce in this contribution.

The total amplitude of the likelihood distributions is not meaningful in the scope of this study. The combined likelihood maps on which we base the following discussion have been presented with brighter shading indicating a higher likelihood over domain boundaries. The scaling of this brighter shading, each map being normalized individually, has been made to facilitate comparison between different geographic areas.

5.2. Correlation With Geological Observations in East Antarctica

The data used for this study are not targeted on shallow geology; however, our findings agree well with crustal boundaries identified from geological field observations, geochronology, and geochemistry (Figure 4). Six major domain boundaries near exposed outcrops have been identified in East Antarctica (reviewed by, e.g., Boger, 2011; Fitzsimons, 2000; Harley et al., 2013). For example, the Shackleton Range is identified with high likelihood to include intersecting major boundaries (Figure 4a), which are indeed seen on the ground or identified subsequently from rock samples (Clarkson et al., 1995; Tessensohn et al.,

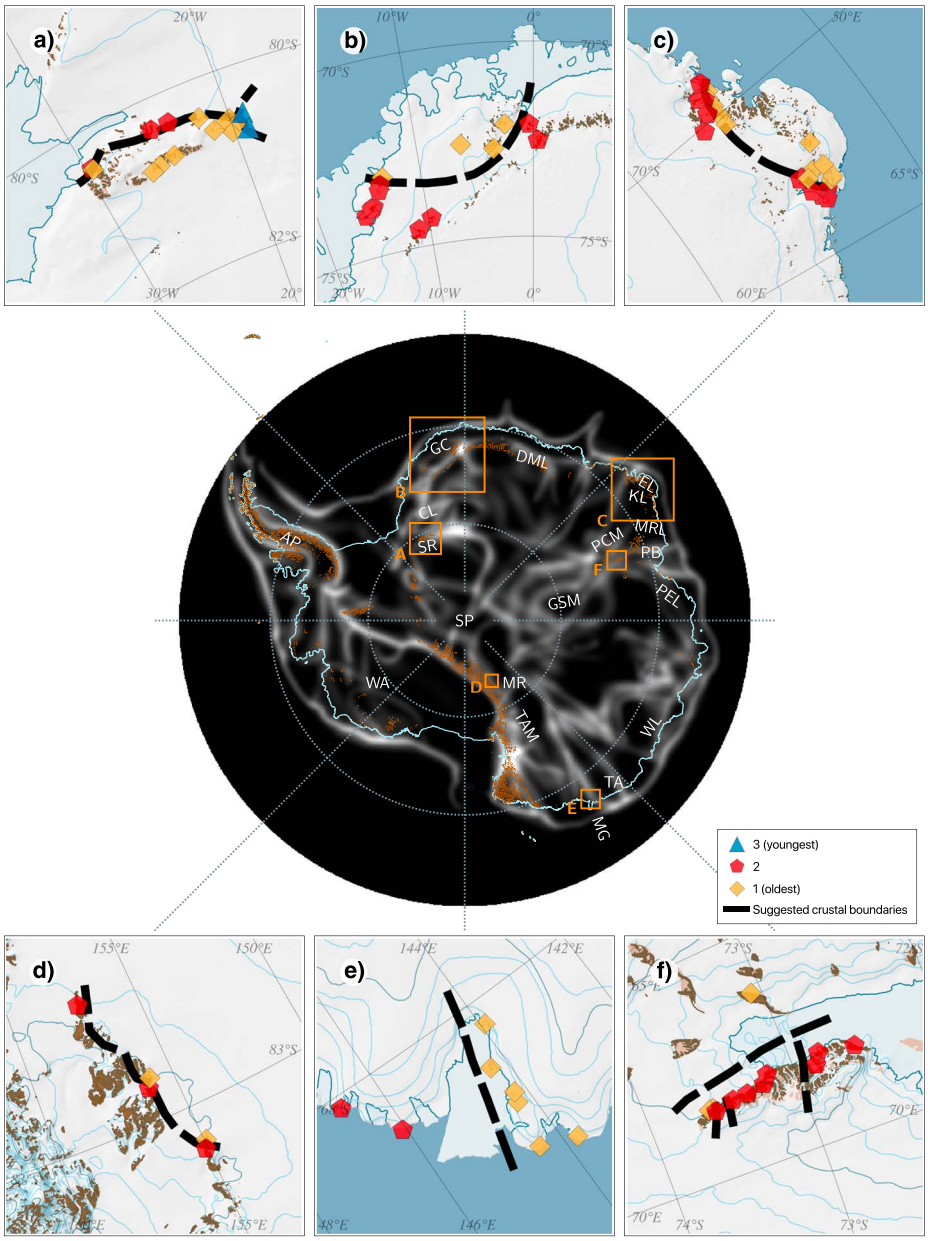

Figure 4. The intersect likelihood map (center, enlarged from Figure 3d) related to major terrane boundaries exposed near outcrops in East Antarctica. (a) Shackleton Range (e.g., Will et al., 2009). A major boundary separating rocks of Archean and younger ages which intersects a further boundary with even younger rocks, east of longitude 20°W. (b) Dronning Maud Land (e.g., Marschall et al., 2010). A boundary between Maud Belt south of Grunehogna Craton. (c) Enderby Land (e.g., Sheraton et al., 1987). The transitional boundary between the Archean and Paleoproterozoic Napier Complex and the reworked Rayner Complex. (d) Miller Range (e.g., Goodge et al., 2001). The boundary between Archean and Paleoproterozoic Nimrod and younger Ross-Delamerian orogenic domains. (e) Mertz Glacier region (e.g., Di Vincenzo et al., 2007). The Archean Terre Adélie Craton is exposed in the west, and Ross-Delamerian domain in the east. (f) Prince Charles Mountains with the Mawson Escarpment (e.g., Boger & Miller, 2004; Corvino et al., 2008; Phillips et al., 2009). This region contains multiple major boundaries currently under debate. Symbols indicate relative ages of examples of geochronological samples from referenced literature. Yellow prisms denote oldest rocks, often Archean. Red pentagons denote younger orogenic rocks. Blue triangles are even younger ages in the Shackleton Range. Black striped lines in insets are geological boundaries modified from original studies for guidance. Brown shade indicates the outline of rock outcrops (Burton-Johnson et al., 2016). AP = Antarctic Peninsula; CL = Coats Land; DML = Dronning Maud Land; EL = Enderby Land; GC = Grunehogna Craton; GSM = Gamburtsev Subglacial Mountains; KL = Kemp Land; MG = Mertz Glacier; MR = Miller Range; MRL = MacRobertson Land; PB = Prydz Bay; PCM = Prince Charles Mountains; PEL = Princess Elizabeth Land; SP = South Pole; SR = Shackleton Range; TA = Terre Adélie; TAM = Transantarctic Mountains; WA = West Antarctica; WL = Wilkes Land.

1999; Will et al., 2009, 2010). The southern boundary of the Archean Grunehogna Craton in Dronning Maud Land (Figure 4b) is identified by our method and agrees well with geological studies (Bauer et al., 2003; Board et al., 2004; Jacobs et al., 1998, 2015; Moyes et al., 1995; Luttinen & Furnes, 2000; Marschall et al., 2010). The Miller Range in the Transantarctic Mountains (Figure 4d) has a high likelihood of a lithospheric domain boundary running along its length. This agrees with geological and geochronological studies as well as magnetic data (Goodge et al., 1992, 2001; Goodge & Finn, 2010). The Mertz Glacier region is also identified with a high likelihood of a major lithospheric boundary (Figure 4e) and matches well with ground observations and subsequent analysis (Di Vincenzo et al., 2007; Lamarque et al., 2016; Ménot et al., 2005, 2007; Peucat et al., 1999; Stuwe & Oliver, 1989). The interpretation of the geology in Prydz Bay area (Figure 4f) is under debate (Boger et al., 2001; Boger & Miller, 2004; Corvino et al., 2008; Fitzsimons, 2000; Kelsey et al., 2008; Phillips et al., 2006, 2009). Notwithstanding the challenges in interpreting the crustal structure, we identify the area with high likelihood for deep lithospheric boundaries. Enderby Land (Figure 4c) contains the Archean and Paleoproterozoic Napier Complex, and the Meso-Neoproterozoic Rayner Complex (Fitzsimons, 2000; Halpin et al., 2007; Kelly, 2002; Kelly & Harley, 2005; Morrissey et al., 2016; Phillips et al., 2009; Sheraton et al., 1980, 1987). We detect the southern boundary of the Napier Complex with a lower likelihood than the exposed locations discussed previously. This complex reworking of MacRobertson Land and Kemp Land (Halpin et al., 2005, 2007; Morrissey et al., 2016) with lithospheric thinning could be the main reason why this particular boundary is less evident from the data sets used.

5.3. Comparison With the Continent of Australia

The approach is also tested for Australia, where the inland geology is better known (supporting information). The Australian example shows that craton boundaries are detected using the multivariate method, but superimposed orogens are more difficult to discern. False detection of major boundaries is unlikely when using a conservative product combination, where all individual likelihood maps must agree (Figure 3e). The Australian example also provides insight into relating surface geological boundaries to deep lithospheric boundaries. Major surface and deep boundaries appear to have a robust mutual association, lending weight to our inferences for East Antarctica. However, we note again that geological boundaries within such continental domains may not have a signature in the deep lithosphere, in particular, for younger lithosphere such as eastern Australia and West Antarctica. Boundaries detected in the deep lithosphere associated with continental extension would not necessarily be seen in the surface geology. We show in the supporting information the extent to which boundaries may be traced between continents in the deep lithosphere.

5.4. New Insights Into the Lithosphere of Antarctica

The new maps that we present enable insights regarding of the nature of the East Antarctic lithosphere to be drawn from geophysical data sets. By combining multiple data sets, in our case three data sets, we manage the possibility of including an arbitrary interpretation. The impact of false detections is mitigated by using accuracy and precision ratings in the calculations that result in the likelihood maps. Our maps show domain boundaries suggesting a complex interior. Coats Land and Dronning Maud Land appear to show lithospheric heterogeneity, while the interior of Wilkes Land is much less segmented, being divided by few boundaries. These suggestions are consistent with more detailed regional studies, where those exist (e.g., Aitken et al., 2014; Jacobs et al., 2015; Ruppel et al., 2018). A complex interior also agrees with recent geological studies that find large age variations in marine cores (Cook et al., 2017), glacial deposits in the Transantarctic Mountains (Goodge, 2018), and what might be expected from other Gondwana continents (e.g., Begg et al., 2009; Korsch & Doublier, 2016; Kennett et al., 2018).

The structure of the lithosphere is the result of its tectonic evolution. With robust constraints for the interior boundaries, we can better infer the nature of the East Antarctic continental assembly. Our likelihood maps suggest that the interior has more domains than shown in previous interpolations as in Figure 1a. For example, it is unlikely that Terre Adélie, Miller Range, and Shackleton Range belong to the same large uninterrupted domain. As a general comment, the extrapolation of major boundaries into the East Antarctic interior seems to be justified for a scale length of approximately 1,000 km. In the interior, at greater than 1,000 km inland, it is very likely that new domains and hence cross-cutting boundaries will be encountered. Possible plate tectonic implications of the newly identified domains are subject of ongoing work. Enigmatic interior domains, with no coastal expression, are highly likely.

Recent studies using different approaches than we present in the current paper also find interior domains or regions. Ebbing et al. (2018) infer a number of domains in the East Antarctic interior from the curvature

index of gravity field with topographic and isostatic correction and suggest the extent of cratonic lithosphere and orogens. Studies that includes both gravity and seismic data also find a heterogenous interior and provide strong arguments to suggest existence of domains (Baranov & Morelli, 2013; Baranov et al., 2017; Pappa et al., 2019). Our contribution complements these studies by providing a method for mapping the boundaries of such domains. The Australian example suggests these hidden domains will be varied, for example, both cratonic and orogenic. Large-scale models of the Antarctic lithosphere (e.g., Haeger et al., 2019) can potentially be further developed from our mapped interior boundaries. Magnetic surveys and Curie depth variations are widely used to investigate the Antarctic crust (e.g., Ferraccioli et al., 2001, 2011; Goodge & Finn, 2010; Martos et al., 2017; Ruppel et al., 2018). While our contribution draws on constraints from the deeper lithosphere, or the asthenosphere where the lithosphere is thin, we plan to incorporate magnetic data in future, regional-scale, multivariate studies with a crustal and upper lithosphere focus.

We hope that our likelihood maps will find wide use in the Antarctic interdisciplinary research community. Three-dimensional glacial isostatic models of the viscosity variations in the lithosphere could incorporate segmentation. Improved knowledge of East Antarctic lithospheric boundaries thus supports future developments in this area. Understanding of the tectonic evolution and crustal segmentation is needed for mapping crustal heat production, as highlighted in a recent study from West Antarctica (Burton-Johnson et al., 2017). With our presented maps, geothermal heat properties from known geology or observations from neighboring Gondwanan continents can be extrapolated into the hidden interior with better confidence for East Antarctica.

Our approach does not limit the number of data sets used, and with additional data sets, the likelihood maps will be further improved as additional data become available. The method can also be applicable on a regional scale, and regional data sets can also be incorporated in continental scale models. Multivariate mapping provides a quantitative, probabilistic, and therefore robust approach for the identification of lithospheric domain boundaries within the East Antarctic interior.

6. Conclusions

We introduce a novel method to combine likelihood maps from independent data sets to estimated locations of lithospheric boundaries in East Antarctica. We find good correlation between our findings and postulated crustal boundaries along the perimeter. The ice-covered interior is heterogeneous and is shown to likely comprise a larger number of distinct domains than suggested by previous work based on extrapolation of observations along the coast. The largest lithospheric domains are likely located in Wilkes Land, Princess Elizabeth Land, and around the South Pole. Coats Land and Dronning Maud Land likely consist of smaller lithospheric domains.

Acknowledgments
Likelihood maps in interoperable formats are archived in the digital data library PANGAEA (https://doi.pangaea.de/10.1594/PANGAEA.901150). Details are provided in the supporting information. We have made use of the following open access data sources: Seismic data are available from the author's web directories (An et al., 2015a). Gravity anomaly data raster (EIGEN-6C4; Förste et al., 2014) and elevation model (BEDMAP2) are obtained as part of the Quantarctica3 GIS package (Roth et al., 2018). The full details of the methodology for reproduction of this research may be found in the provided SCons script (Knight, 2005). We thank the anonymous reviewers whose comments have greatly improved this manuscript. This research was supported under Australian Research Council's Special Research Initiative for Antarctic Gateway Partnership (Project ID SR140300001). The authors declare that they have no conflict of interest.

References

Aitken, A. R. A., Young, D. A., Ferraccioli, F., Betts, P. G., Greenbaum, J. S., Richter, T. G., et al. (2014). The subglacial geology of Wilkes Land, East Antarctica. *Geophysical Research Letters*, *41*, 2390–2400. https://doi.org/10.1002/2014GL059405

An, M. (2012). A simple method for determining the spatial resolution of a general inverse problem. *Geophysical Journal International*, *191*(2), 849–864. https://doi.org/10.1111/j.1365-246x.2012.05661.x

An, M., Wiens, D. A., Zhao, Y., Feng, M., Nyblade, A., Kanao, M., et al. (2015b). Temperature, lithosphere-asthenosphere boundary and heat flux beneath the Antarctic Plate inferred from seismic velocities. *Journal of Geophysical Research: Solid Earth*, *119*, 8720–8742. https://doi.org/10.1002/2015jb011917

An, M., Wiens, D. A., Zhao, Y., Feng, M., Nyblade, A. A., Kanao, M., et al. (2015a). S-velocity model and inferred Moho topography beneath the Antarctic Plate from Rayleigh waves. *Journal of Geophysical Research: Solid Earth*, *120*, 2007–2010. https://doi.org/10.1002/2014jb011332

Baranov, A., & Morelli, A. (2013). The Moho depth map of the Antarctica region. *Tectonophysics*, *609*, 299–313. https://doi.org/10.1016/j.tecto.2012.12.023

Baranov, A., Tenzer, R., & Bagherbandi, M. (2017). Combined gravimetric–seismic crustal model for Antarctica. *Surveys in Geophysics*, *39*(1), 23–56. https://doi.org/10.1007/s10712-017-9423-5

Bauer, W., Jacobs, J., Fanning, C. M., & Schmidt, R. (2003). Late Mesoproterozoic arc and back-arc volcanism in the Heimefrontfjella (East Antarctica) and implications for the palaeogeography at the southeastern margin of the Kaapvaal-Grunehogna Craton. *Gondwana Research*, *6*(3), 449–465. https://doi.org/10.1016/s1342-937x(05)70998-9

Begg, G. C., Griffin, W. L., Natapov, L. M., O'Reilly, S. Y., Grand, S. P., O'Neill, C. J., et al. (2009). The lithospheric architecture of Africa: Seismic tomography, mantle petrology, and tectonic evolution. *Geosphere*, *5*(1), 23–50. https://doi.org/10.1130/ges00179.1

Block, A. E., Bell, R. E., & Studinger, M. (2009). Antarctic crustal thickness from satellite gravity: Implications for the Transantarctic and Gamburtsev Subglacial Mountains. *Earth and Planetary Science Letters*, *288*(1-2), 194–203. https://doi.org/10.1016/j.epsl.2009.09.022

Board, W. S., Frimmel, H. E., & Aa, R. A. (2004). Pan-African tectonism in the western Maud Belt: P–T–t path for high-grade gneisses in the H.U. Sverdrupfjella, East Antarctica. *Journal of Petrology*, *46*(4), 671–699. https://doi.org/10.1093/petrology/egh093

Boger, S. D. (2011). Antarctica—Before and after Gondwana. *Gondwana Research*, *19*(2), 335–371. https://doi.org/10.1016/j.gr.2010.09.003

Boger, S. D., & Miller, J. M. (2004). Terminal suturing of Gondwana and the onset of the Ross-Delamerian Orogeny: The cause and effect of an Early Cambrian reconfiguration of plate motions. *Earth and Planetary Science Letters*, *219*(1-2), 35–48. https://doi.org/10.1016/S0012-821X(03)00692-7

Boger, S. D., Wilson, C. J. L., & Fanning, C. M. (2001). Early Paleozoic tectonism within the East Antarctic craton: The final suture between east and west Gondwana? *Geology*, *29*(5), 463–466. https://doi.org/10.1130/0091-7613(2001)029h0463:eptwtei2.0.co;2

Brualdi, R. A. (1992). *Introductory combinatorics* (Vol. 3). New York: Pearson Education.

Burton-Johnson, A., Black, M., Fretwell, P. T., & Kaluza-Gilbert, J. (2016). An automated methodology for differentiating rock from snow, clouds and sea in Antarctica from Landsat 8 imagery: A new rock outcrop map and area estimation for the entire Antarctic continent. *The Cryosphere*, *10*(4), 1665–1677. https://doi.org/10.5194/tc-10-1665-2016

Burton-Johnson, A., Halpin, J. A., Whittaker, J. M., Graham, F. S., & Watson, S. J. (2017). A new heat flux model for the Antarctic Peninsula incorporating spatially variable upper crustal radiogenic heat production. *Geophysical Research Letters*, *44*, 5436–5446. https://doi.org/10.1002/2017gl073596

Chaput, J., Aster, R. C., Huerta, A., Sun, X., Lloyd, A., Wiens, D., et al. (2014). The crustal thickness of West Antarctica. *Journal of Geophysical Research: Solid Earth*, *119*, 378–395. https://doi.org/10.1002/2013JB010642

Clarkson, P. D., Tessensohn, F., & Thomson, J. W. (1995). *Geological map of the Shackleton Range, Antarctica*, BAS GEOMAP. Cambridge: British Antarctic Survey.

Cook, C. P., Hemming, S. R., van de Flierdt, T., Davis, E. L. P., Williams, T., Galindo, A. L., et al. (2017). Glacial erosion of East Antarctica in the Pliocene: A comparative study of multiple marine sediment provenance tracers. *Chemical Geology*, *466*, 199–218. https://doi.org/10.1016/j.chemgeo.2017.06.011

Corvino, A. F., Boger, S. D., Henjes-Kunst, F., Wilson, C. J. L., & Fitzsimons, I. C. W. (2008). Superimposed tectonic events at 2450Ma, 2100Ma, 900Ma and 500Ma in the North Mawson Escarpment, Antarctic Prince Charles Mountains. *Precambrian Research*, *167*(3-4), 281–302. https://doi.org/10.1016/j.precamres.2008.09.001

Craddock, C. (1972). *Antarctic tectonics* (pp. 449–455). Oslo: Antarctic geology and geophysics. Universitetsforlaget.

Daczko, N. R., Halpin, J. A., Fitzsimons, I. C. W., & Whittaker, J. M. (2018). A cryptic Gondwana-forming orogen located in Antarctica. *Scientific Reports*, *8*(1). https://doi.org/10.1038/s41598-018-26530-1

Di Vincenzo, G., Talarico, F., & Kleinschmidt, G. (2007). An 40 Ar–39 Ar investigation of the Mertz Glacier area (George V Land, Antarctica): Implications for the Ross Orogen–East Antarctic Craton relationship and Gondwana reconstructions. *Precambrian Research*, *152*(3), 93–118. https://doi.org/10.1016/j.precamres.2006.10.002

Ebbing, J., Haas, P., Ferraccioli, F., Pappa, F., Szwillus, W., & Bouman, J. (2018). Earth tectonics as seen by GOCE—Enhanced satellite gravity gradient imaging. *Scientific Reports*, *8*(1). https://doi.org/10.1038/s41598-018-34733-9

Ferraccioli, F., Coren, F., Bozzo, E., Zanolla, C., Gandolfi, S., Tabacco, I., & Frezzotti, M. (2001). Rifted(?) crust at the East Antarctic Craton margin: Gravity and magnetic interpretation along a traverse across the Wilkes Subglacial Basin region. *Earth and Planetary Science Letters*, *192*(3), 407–421. https://doi.org/10.1016/S0012-821X(01)00459-9

Ferraccioli, F., Finn, Carola., Jordan, T., Bell, R. E., Anderson, L., & Damaske, S. (2011). East Antarctic rifting triggers uplift of the Gamburtsev Mountains. *Nature*, *479*(7373), 388–392. https://doi.org/10.1038/nature10566

Fitzsimons, I. C. W. (2000). Grenville-age basement provinces in East Antarctica: Evidence for three separate collisional orogens. *Geology*, *28*(10), 879–882.

Fitzsimons, I. C. W. (2000). A review of tectonic events in the East Antarctic Shield and their implications for Gondwana and earlier supercontinents. *Journal of African Earth Sciences*, *31*(1), 3–23. https://doi.org/10.1016/S0899-5362(00)00069-5

Fitzsimons, I. C. W. (2003). Proterozoic basement provinces of southern and southwestern Australia, and their correlation with Antarctica. *Geological Society, London, Special Publications*, *206*(1), 93–130. https://doi.org/10.1144/GSL.SP.2003.206.01.07

Förste, C., Bruinsma, S. L., Abrikosov, O., Lemoine, J.-M., Marty, J. C., Flechtner, F., et al. (2014). EIGEN-6C4 The latest combined global gravity field model including GOCE data up to degree and order 2190 of GFZ Potsdam and GRGS Toulouse, GFZ Data Services.

Foulger, G. R., Panza, G. F., Artemieva, I. M., Bastow, I. D., Cammarano, F., Evans, J. R., et al. (2013). Caveats on tomographic images. *Terra Nova*, *25*(4), 259–281.

Fretwell, P., Pritchard, H. D., Vaughan, D. G., Bamber, J. L., Barrand, N. E., Bell, R., et al. (2013). Bedmap2: Improved ice bed, surface and thickness datasets for Antarctica. *The Cryosphere*, *7*(1), 375–393. https://doi.org/10.5194/tcd-6-4305-2012

Gillies, S. (2018). Rasterio: Geospatial raster I/O for Python programmers. Retrieved from https://github.com/mapbox/rasterio

Goodge, J. W. (2018). Crustal heat production and estimate of terrestrial heat flow in central East Antarctica, with implications for thermal input to the East Antarctic ice sheet. *The Cryosphere*, *12*(2), 491–504. https://doi.org/10.5194/tc-12-491-2018

Goodge, J. W., Fanning, C. M., & Bennett, V. C. (2001). U-Pb evidence of 1.7 Ga crustal tectonism during the Nimrod Orogeny in the Transantarctic Mountains, Antarctica: Implications for Proterozoic plate reconstructions. *Precambrian Research*, *112*(3-4), 261–288. https://doi.org/10.1016/S0301-9268(01)00193-0

Goodge, J. W., & Finn, C. A. (2010). Glimpses of East Antarctica: Aeromagnetic and satellite magnetic view from the central transantarctic mountains of East Antarctica. *Journal of Geophysical Research*, *115*, B09103. https://doi.org/10.1029/2009JB006890

Goodge, J. W., Hansen, V. L., & Peacock, S. M. (1992). *Multiple petrotectonic events in high-grade metamorphic rocks of the Nimrod Group, central Transantarctic Mountains, Antarctica* (pp. 203–209). Tokyo: Recent Progress in Antarctic Earth Science. Terra Scientific.

Graham, F. S., Roberts, J. L., Galton-Fenzi, B. K., Young, D., Blankenship, D., & Siegert, M. J. (2017). A high-resolution synthetic bed elevation grid of the Antarctic continent. *Earth System Science Data*, *9*(1), 267–279. https://doi.org/10.5194/essd-9-267-2017

Gregory R. B., Samantha E. H., & Yongcheol P. (2017). Variable thermal loading and flexural uplift along the Transantarctic Mountains, Antarctica. *Geology*, *45*(5), 463–466. https://doi.org/10.1130/g38784.1

Haeger, C., Kaban, M. K., Tesauro, M., Petrunin, A. G., & Mooney, W. D. (2019). 3D density, thermal and compositional model of the antarctic lithosphere and implications for its evolution. *Geochemistry, Geophysics, Geosystems*, *20*, 688–707. https://doi.org/10.1029/2018GC008033

Halpin, J. A., Clarke, G. L., White, R. W., & Kelsey, D. E. (2007). Contrasting P–T–t paths for Neoproterozoic metamorphism in MacRobertson and Kemp Lands, East Antarctica. *Journal of Metamorphic Geology*, *25*(6), 683–701. https://doi.org/10.1111/j.1525-1314.2007.00723.x

Halpin, J. A., Gerakiteys, C. L., Clarke, G. L., Belousova, E. A., & Griffin, W. L. (2005). In-situ UPb geochronology and Hf isotope analyses of the Rayner Complex, east Antarctica. *Contributions to Mineralogy and Petrology*, *148*(6), 689–706. https://doi.org/10.1007/s00410-004-0627-6

Hansen, S. E., Nyblade, A. A., Heeszel, D. S., Wiens, D. A., Shore, P., & Kanao, M. (2010). Crustal structure of the Gamburtsev Mountains, East Antarctica, from S-wave receiver functions and Rayleigh wave phase velocities. *Earth and Planetary Science Letters*, *300*(3-4), 395–401. https://doi.org/10.1016/j.epsl.2010.10.022

Harley, S. L., Fitzsimons, I. C. W., & Zhao, Y. (2013). Antarctica and supercontinent evolution: historical perspectives, recent advances and unresolved issues. *Geological Society, London, Special Publications*, *383*(1), 1–34. https://doi.org/10.1144/SP383.9

Heeszel, D. S., Wiens, D. A., Anandakrishnan, S., Aster, R. C., Dalziel, I. W. D., Huerta, A. D., et al. (2016). Upper mantle structure of central and West Antarctica from array analysis of Rayleigh wave phase velocities. *Journal of Geophysical Research: Solid Earth*, *121*, 1758–1775. https://doi.org/10.1002/2015jb012616

Jacobs, J., Elburg, M., Läufer, A., Kleinhanns, I. C., Henjes-Kunst, F., Estrada, S., et al. (2015). Two distinct Late Mesoproterozoic/Early Neoproterozoic basement provinces in central/eastern Dronning Maud Land, East Antarctica: The missing link, 15 -21° E. *Precambrian Research*, *265*, 249–272. https://doi.org/10.1016/j.precamres.2015.05.003

Jacobs, J., Fanning, C. Mark, Henjes-Kunst, F., Olesch, M., & Paech, H.-J. (1998). Continuation of the Mozambique Belt into East Antarctica: Grenville age metamorphism and polyphase Pan African high grade events in central Dronning Maud Land. *The Journal of Geology*, *106*(4), 385–406. https://doi.org/10.1086/516031

Jordan H. G., Samantha E. H., Charles A. L., Brian A. Y., Akram M., & Yongcheol P. (2017). An assessment of crustal and upper-mantle velocity structure by removing the effect of an ice layer on the P-wave response: An application to Antarctic seismic studies. *Bulletin of the Seismological Society of America*, *107*(2), 639–651. https://doi.org/10.1785/0120160262

Kaufmann, G., Wu, P., & Ivins, E. R. (2005). Lateral viscosity variations beneath Antarctica and their implications on regional rebound motions and seismotectonics. *Journal of Geodynamics*, *39*(2), 165–181. https://doi.org/10.1016/j.jog.2004.08.009

Kelly, N. M. (2002). A two-stage evolution of the Neoproterozoic Rayner Structural Episode: New UPb sensitive high resolution ion microprobe constraints from the Oygarden Group, Kemp Land, East Antarctica. *Precambrian Research*, *116*(3-4), 307–330. https://doi.org/10.1016/s0301-9268(02)00028-1

Kelly, N. M., & Harley, S. L. (2005). An integrated microtextural and chemical approach to zircon geochronology: Refining the Archaean history of the Napier Complex, east Antarctica. *Contributions to Mineralogy and Petrology*, *149*(1), 57–84. https://doi.org/10.1007/s00410-004-0635-6

Kelsey, D. E., Wade, B. P., Collins, A. S., Hand, M., Sealing, C. R., & Netting, A. (2008). Discovery of a Neoproterozoic basin in the Prydz belt in East Antarctica and its implications for Gondwana assembly and ultrahigh temperature metamorphism. *Precambrian Research*, *161*(3–4), 355–388. https://doi.org/10.1016/j.precamres.2007.09.003

Kennett, B. L. N. (2005). *Seismological tables: AK135* (pp. 1–289). Australia: Research School of Earth Sciences, Australian National University Canberra.

Kennett, B. L. N., Chopping, R., & Blewett, R. (2018). *The Australian continent: A geophysical synthesis*: ANU Press and Commonwealth of Australia (Geoscience Australia).

Knight, S. (2005). Building software with SCons. *Computing in Science & Engineering*, *7*(1), 79–88. https://doi.org/10.1109/MCSE.2005.11

Korsch, R. J., & Doublier, M. P. (2016). Major crustal boundaries of Australia, and their significance in mineral systems targeting. *Ore Geology Reviews*, *76*, 211–228. https://doi.org/10.1016/j.oregeorev.2015.05.010

Lamarque, G., Bascou, J., Maurice, C., Cottin, J.-Y., Riel, N., & Ménot, R.-P. (2016). Microstructures, deformation mechanisms and seismic properties of a Palaeoproterozoic shear zone: The Mertz shear zone, East-Antarctica. *Tectonophysics*, *680*, 174–191. https://doi.org/10.1016/j.tecto.2016.05.011

Laske, G., Masters, G., Ma, Z., & Pasyanos, M. (2013). Update on crust1. 0a 1-degree global model of earthscrust, *Geophys. res. abstr* (pp. 2658). Austria: EGU General Assembly Vienna.

Leitchenkov, G. L., Antonov, A. V., Luneov, P. I., & Lipenkov, V. Y. (2016). Geology and environments of subglacial lake Vostok. *Philosophical Transactions of the Royal Society A: Mathematical, Physical and Engineering Sciences*, *374*(2059), 20140302.

Luttinen, A. V., & Furnes, H. (2000). Flood basalts of Vestfjella: Jurassic magmatism across an Archaean-Proterozoic lithospheric boundary in Dronning Maud Land, Antarctica. *Journal of Petrology*, *41*(8), 1271–1305. https://doi.org/10.1093/petrology/41.8.1271

Marschall, H. R., Hawkesworth, C. J., Storey, C. D., Dhuime, B., Leat, P. T., Meyer, H.-P., & Tamm-Buckle, S. (2010). The Annandagstoppane Granite, East Antarctica: Evidence for Archaean Intracrustal Recycling in the Kaapvaal-Grunehogna Craton from Zircon O and Hf Isotopes. *Journal of Petrology*, *51*(11), 2277–2301. https://doi.org/10.1093/petrology/egq057

Martos, Y. M., Catalán, M., Jordan, T. A., Golynsky, A., Golynsky, D., Eagles, G., & Vaughan, D. G. (2017). Heat flux distribution of Antarctica unveiled. *Geophysical Research Letters*, *44*, 11,417–11,426. https://doi.org/10.1002/2017gl075609

Ménot, R. P., Duclaux, G., Peucat, J. J., Rolland, Y., Guillot, S., Fanning, M., et al. (2007). Geology of the Terre Adelie craton (135–146 E). In A. K. Cooper, C. R. Raymond, & et al. (Eds.), *Antarc-ica: A Keystone in a Changing World-Online Proceedings of the 10th 590 ISAES* (Vol. 1047). USGS Open-File Report. https://doi.org/10.3133/592ofr20071047srp048

Ménot, R.-P., Pecher, A., Rolland, Y., Peucat, J. J., Pelletier, A., Duclaux, G., & Guillot, S. (2005). Structural Setting of the Neoarchean Terrains in the Commonwealth Bay Area (143-145E), Terre Adelie Craton, East Antarctica. *Gondwana Research*, *8*(1), 1–9. https://doi.org/10.1016/s1342-937x(05)70258-6

Morrissey, L. J., Hand, M., Kelsey, D. E., & Wade, B. P. (2016). Cambrian high-temperature reworking of the Rayner–eastern Ghats terrane: Constraints from the northern Prince Charles Mountains region, East Antarctica. *Journal of Petrology*, *57*(1), 53–92. https://doi.org/10.1093/petrology/egv082

Moyes, A. B., Krynauw, J. R., & Barton, J. M. (1995). The age of the Ritscherflya Supergroup and Borgmassivet intrusions, Dronning Maud Land, Antarctica. *Antarctic Science*, *7*(1), 87. https://doi.org/10.1017/s0954102095000125

Pail, R., Goiginger, H., Schuh, W. D., Höck, E., Brockmann, J. M., Fecher, T., et al. (2010). Combined satellite gravity field model GOCO01S derived from GOCE and GRACE. *Geophysical Research Letters*, *37*, L20314. https://doi.org/10.1029/2010GL044906

Pappa, F., Ebbing, J., & Ferraccioli, F. (2019). Moho depths of antarctica: Comparison of seismic, gravity, and isostatic results. *Geochemistry, Geophysics, Geosystems*, *20*, 1629–1645. https://doi.org/10.1029/2018GC008111

Pasyanos, M. E., Masters, T. G., Laske, G., & Ma, Z. (2014). LITHO1. 0: An updated crust and lithospheric model of the Earth. *Journal of Geophysical Research: Solid Earth*, *119*, 2153–2173. https://doi.org/10.1002/2013jb010626

Peucat, J. J., Ménot, R. P., Monnier, O., & Fanning, C. M. (1999). The Terre Adelie basement in the East-Antarctica Shield: Geological and isotopic evidence for a major 1.7 Ga thermal event; comparison with the Gawler Craton in South Australia. *Precambrian Research*, *94*(3-4), 205–224. https://doi.org/10.1016/S0301-9268(98)00119-3

Phillips, G., Kelsey, D. E., Corvino, A. F., & Dutch, R. A. (2009). Continental reworking during overprinting orogenic events, southern Prince Charles Mountains, East Antarctica. *Journal of Petrology*, *50*(11), 2017–2041. https://doi.org/10.1093/petrology/egp065

Phillips, G., Wilson, C. J. L., Campbell, I. H., & Allen, C. M. (2006). U–Th–Pb detrital zircon geochronology from the southern Prince Charles mountains, east Antarctica—defining the Archaean to Neoproterozoic Ruker province. *Precambrian Research*, *148*(3), 292–306. https://doi.org/10.1016/j.precamres.2006.05.001

Pollard, D., DeConto, R. M., & Nyblade, A. A. (2005). Sensitivity of Cenozoic Antarctic ice sheet variations to geothermal heat flux. *Global and Planetary Change*, *49*(1–2), 63–74. https://doi.org/10.1016/j.gloplacha.2005.05.003

QGIS (2015). QGIS geographic information system, Open Source Geospatial Foundation Project (By development team and community).

Ravich, M. G., Klimov, L. V., & Solovev, D. S. (1965). *Dokembriy Vostochnoy Antarktidy (The Precambrian of East Antarctica)* (Vol. 658). Moskva: Izdatel'stvo Nedra.

Reading, A. M. (2006). The seismic structure of Precambrian and early Palaeozoic terranes in the Lambert Glacier region, East Antarctica. *Earth and Planetary Science Letters*, *244*(1–2), 44–57. https://doi.org/10.1016/j.epsl.2006.01.031

Reading, A. M. (2007). The seismicity of the Antarctic plate. *The Geological Society of America Special Paper*, *425*(18), 285–298. https://doi.org/10.1130/2007.2425(18)

Ritsema, J., Van Heijst, H. J., & Woodhouse, J. H. (2004). Global transition zone tomography. *Journal of Geophysical Research*, *109*, B02302. https://doi.org/10.1029/2003JB002610

Ritzwoller, M. H., Shapiro, N. M., Barmin, M. P., & Levshin, A. L. (2002). Global surface wave diffraction tomography. *Journal of Geophysical Research*, *107*(B12), 2335.

Ritzwoller, M. H., Shapiro, N. M., Levshin, A. L., & Leahy, G. M. (2001). Crustal and upper mantle structure beneath Antarctica and surrounding oceans. *Journal Of Geophysical Research*, *106*(12), 30,645–30,670.

Roth, G., Matsuoka, K., Skoglund, A., Melvær, Y., & Tronstad, S. (2018). Quantarctica: A unique, open, standalone GIS package for Antarctic research and education. Retrieved from http://quantarctica.npolar.no

Roult, G., & Rouland, D. (1994). Antarctica I: Deep structure investigations inferred from seismology: A review. *Physics of the Earth and Planetary Interiors*, *84*(1–4), 15–32. https://doi.org/10.1016/0031-9201(94)90032-9

Roult, G., Rouland, D., & Montagner, J. P. (1994). Antarctica II: Upper-mantle structure from velocities and anisotropy. *Physics of the Earth and Planetary Interiors*, *84*(1–4), 33–57. https://doi.org/10.1016/0031-9201(94)90033-7

Ruppel, A., Jacobs, J., Eagles, G., Läufer, A., & Jokat, W. (2018). New geophysical data from a key region in East Antarctica: Estimates for the spatial extent of the Tonian Oceanic Arc Super Terrane (TOAST). *Gondwana Research*, *59*, 97–107. https://doi.org/10.1016/j.gr.2018.02.019

Schaeffer, A. J., & Lebedev, S. (2015). Global heterogeneity of the lithosphere and underlying mantle: A seismological appraisal based on multimode surface-wave dispersion analysis, shear-velocity tomography, and tectonic regionalization. In *The Earth's heterogeneous mantle* (pp. 3–46). Cham: Springer International Publishing. https://doi.org/10.1007/978-3-319-15627-91

Shapiro, N. M., & Ritzwoller, M. H. (2002). Monte-Carlo inversion for a global shear-velocity model of the crust and upper mantle. *Geophysical Journal International*, *151*(1), 88–105.

Shen, W., Wiens, D. A., Anandakrishnan, S., Aster, R. C., Gerstoft, P., Bromirski, P. D., et al. (2018). The crust and upper mantle structure of Central and West Antarctica From Bayesian inversion of rayleigh wave and receiver functions. *Journal of Geophysical Research: Solid Earth*, *123*, 7824–7849. https://doi.org/10.1029/2017JB015346

Shen, W., Wiens, D. A., Stern, T., Anandakrishnan, S., Aster, R. C., Dalziel, I., et al. (2017). Seismic evidence for lithospheric foundering beneath the southern Transantarctic Mountains, Antarctica. *Geology*, *46*(1), 71–74. https://doi.org/10.1130/g39555.1

Sheraton, J. W., Offe, L. A., Tingey, R. J., & Ellis, D. J. (1980). Enderby Land, Antarctica—An unusual Precambrian high-grade metamorphic terrain. *Journal of the Geological Society of Australia*, *27*(1–2), 1–18.

Sheraton, J. W., Tingey, R. J., Black, L. P., Offe, L. A., & Ellis, D. J. (1987). Geology of an unusual Precambrian high-grade metamorphic terrane-Enderby Land and western Kemp Land, Antarctica. *Australian Bureau of Mineral Resources Bulletin*, *223*.

Stuwe, K., & Oliver, R. (1989). Geological history of Adelie-Land and King-George-V-Land, Antarctica—Evidence for a Polycyclic Metamorphic Evolution. *Precambrian Research*, *43*(4), 317–334.

Tauxe, L., Sugisaki, S., Jiménez-Espejo, F., Escutia, C., Cook, C. P., van de Flierdt, T., & Iwai, M. (2015). Geology of the Wilkes land sub-basin and stability of the East Antarctic ice sheet: Insights from rock magnetism at IODP site U1361. *Earth and Planetary Science Letters*, *412*, 61–69. https://doi.org/10.1016/j.epsl.2014.12.034

Tessensohn, F., Kleinschmidt, G., Talarico, F., Buggisch, W., Brommer, A., Henjes-Kunst, F., et al. (1999). Ross-age amalgamation of East and West Gondwana: Evidence from the Shackleton Range, Antarctica. *Terra Antartica*, *6*(3-4), 317–325.

Tingey, R. J. (1991). *The geology of Antarctica*, No. 17. USA: Oxford University Press. https://doi.org/10.1029/GM007p0026

Veevers, J. J. (2012). Reconstructions before rifting and drifting reveal the geological connections between Antarctica and its conjugates in Gondwanaland. *Earth-Science Reviews*, *111*(3), 249–318. https://doi.org/10.1016/j.earscirev.2011.11.009

Visser, P. N. A. M. (1999). Gravity field determination with GOCE and GRACE. *Advances in Space Research*, *23*(4), 771–776.

Whitehouse, P. L. (2018). Glacial isostatic adjustment modelling: Historical perspectives, recent advances, and future directions. *Earth Surface Dynamics*, *6*(2), 401–429. https://doi.org/10.5194/esurf-6-401-2018

Whitehouse, P. L., Latychev, K., Milne, G. A., Mitrovica, J. X., & Kendall, R. (2006). Impact of 3-D Earth structure on Fennoscandian glacial isostatic adjustment: Implications for space-geodetic estimates of present-day crustal deformations. *Geophysical Research Letters*, *33*, L13502. https://doi.org/10.1029/2006GL026568

Will, T. M., Frimmel, H. E., Zeh, A., Le Roux, P., & Schmädicke, E. (2010). Geochemical and isotopic constraints on the tectonic and crustal evolution of the Shackleton Range, East Antarctica, and correlation with other Gondwana crustal segments. *Precambrian Research*, *180*(1–2), 85–112. https://doi.org/10.1016/j.precamres.2010.03.005

Will, T. M., Zeh, A., Gerdes, A., Frimmel, H. E., Millar, I. L., & Schmädicke, E. (2009). Palaeoproterozoic to Palaeozoic magmatic and metamorphic events in the Shackleton Range, East Antarctica: Constraints from zircon and monazite dating, and implications for the amalgamation of Gondwana. *Precambrian Research*, *172*(1–2), 25–45. https://doi.org/10.1016/j.precamres.2009.03.008

Winberry, J. P., & Anandakrishnan, S. (2004). Crustal structure of the West Antarctic rift system and Marie Byrd Land hotspot. *Geology*, *32*(11), 977. https://doi.org/10.1130/g20768.1

References From the Supporting Information

Bacchin, M., Milligan, P. R., Wynne, P., & Tracey, R. (2008). *Gravity anomaly map of the Australian region, scale 1: 5 000 000*. Canberra: Geoscience Australia. Retrieved from https://researchdata.ands.org.au/gravity-anomaly-map-edition-2008/1288642?source=suggesteddatasets

Betts, P. G., Giles, D., Lister, G. S., & Frick, L. R. (2002). Evolution of the Australian lithosphere. *Australian Journal of Earth Sciences*, *49*(4), 661–695. https://doi.org/10.1046/j.1440-0952.2002.00948.x

Boyden, J. A., Müller, R. D., Gurnis, M., Torsvik, T. H., Clark, J. A., Turner, M., et al. (2011). Next-generation plate-tectonic reconstructions using GPlates.

Cawood, P. A., & Korsch, R. (2008). Assembling australia: Proterozoic building of a continent. *Precambrian Research*, *166*(1-4), 1–35. https://doi.org/10.1016/j.precamres.2008.08.006

Craddock, C. (1970). *Tectonic map of Antarctica*: American Geographical Society Antarctic Map Folio series Folio 12 - Geology, Plate XXI.

Geoscience Australia (2017). Digital Elevation Model (DEM) Shuttle radar Topography Mission (SRTM) 1 Second over Australian Bathymetry Topography WCS. *Geoscience Australia*. Retrieved from http://pid.geoscience.gov.au/service/ga/100320

Kennett, B. L. N., Fichtner, A., Fishwick, S., & Yoshizawa, K. (2012). Australian Seismological Reference Model (AuSREM): Mantle component. *Geophysical Journal International*, *192*(2), 871–887. https://doi.org/10.1093/gji/ggs065

Liu, Y., Li, Z.-X., Pisarevsky, S. A., Kirscher, U., Mitchell, R. N., Stark, J. Camilla, et al. (2018). First precambrian palaeomagnetic data from the Mawson craton (East Antarctica) and tectonic implications. *Scientific Reports*, *8*(1), 16403. https://doi.org/10.1038/s41598-018-34748-2

Matthews, K. J., Maloney, K. T., Zahirovic, S., Williams, S. E., Seton, M., & Müller, R. D. (2016). Global plate boundary evolution and kinematics since the late Paleozoic. *Global and Planetary Change*, *146*, 226–250. https://doi.org/10.1016/j.gloplacha.2016.10.002

Morrissey, L. J., Payne, J. L., Hand, M., Clark, C., Taylor, R., Kirkland, C. L., & Kylander-Clark, A. (2017). Linking the Windmill Islands, East Antarctica and the Albany–Fraser Orogen: Insights from U–Pb zircon geochronology and Hf isotopes. *Precambrian Research*, *293*, 131–149. https://doi.org/10.1016/j.precamres.2017.03.005

Myers, J. S., Shaw, R. D., & Tyler, I. M. (1996). Tectonic evolution of Proterozoic Australia. *Tectonics*, *15*(6), 1431–1446. https://doi.org/10.1029/96tc02356

Shaw, R. D., Wellman, P., Gunn, P., Whitaker, A. J., Tarlowski, C., & Morse, M. P. (1995). Australian crustal elements map. *AGSO Research Newsletter*, *23*, 1–3.